Novel ceramides recovered from *Porphyromonas gingivalis*: relationship to adult periodontitis

Frank C. Nichols

Department of Periodontology, University of Connecticut School of Dental Medicine, 263 Farmington Avenue, Farmington, CT 06030

Abstract **The primary purpose of this study was to characterize the major structural features of ceramides recovered from *Porphyromonas gingivalis*, a suspected periodontal pathogen. Complex lipids extracted from *P. gingivalis* were treated with N,O-bis(trimethylsilyl)-trifluoroacetamide and analyzed using gas chromatography–mass spectrometry. Mass spectra of lipid derivatives revealed cleavage products consistent with structures of four major ceramides. Two of the major ceramides are proposed to contain long chain bases of either 2-amino-1,3-octadecanediol or 2-amino-1,3-nonadecanediol in amide linkage to 3-hydroxy *iso*branched $C_{17:0}$. The remaining major ceramides are proposed to contain either 2-amino-1,3-octadecanediol or 2-amino-1,3-nonadecanediol in amide linkage to $C_{17:1}$. Alkaline hydrolysis of *P. gingivalis* lipids and subsequent formation of suitable derivatives revealed 3-hydroxy *iso*branched $C_{17:0}$, $C_{17:1}$, 2-amino-1,3-octadecanediol, and 2-amino-1,3-nonadecanediol as hydrolysis products. Therefore, the constitutive fatty acids and long chain bases recovered in alkaline hydrolysis products of *P. gingivalis* lipids are consistent with the proposed ceramide structures. The next goal of this study was to investigate whether these bacterial ceramides exist in lipid extracts of human teeth and gingival tissue at sites of severe adult periodontitis. Using selected ion monitoring of characteristic ions and retention times for each ceramide described above, lipids from teeth and gingival tissue were shown to contain primarily the ceramides containing $C_{17:1}$. It is concluded that *P. gingivalis* synthesizes at least four major ceramides and two of these ceramides are selectively adsorbed to diseased tooth surfaces and may penetrate into diseased gingival tissue.—**Nichols, F. C. **Novel ceramides recovered from *Porphyromonas gingivalis*: relationship to adult periodontitis. *J. Lipid Res.* 1998.** 39: **2360–2372.**

Supplementary key words *Porphyromonas gingivalis* • long chain bases • tooth lipids • gas chromatography–mass spectrometry

At least three genera of gram-negative organisms, including *Bacteroides*, *Porphyromonas*, and *Prevotella*, synthesize 3-hydroxy *iso*branched $C_{17:0}$ as well as other hydroxy and branched-chain fatty acids (1–4). Of these organisms, specific strains of *Bacteroides* were shown to incorporate at least half of the total 3-hydroxy *iso*branched $C_{17:0}$ into complex lipids other than lipopolysaccharide with the majority of the lipid-associated 3-hydroxy *iso*branched $C_{17:0}$ held in amide linkage to complex lipids (5, 6). Additional reports demonstrated the capacity of *Bacteroides* to synthesize ceramide phospholipids (7–11) which contain fatty acid in amide linkage. Hydrolysis of ceramide phospholipids and other sphingolipids of *Bacteroides melaninogenicus* released three long chain bases as defined by White, Tucker, and Sweeley (12). However, the structures of ceramide phospholipids, including their fatty acid constituents, produced by *Bacteroides* sp. remain to be verified.

Porphyromonas gingivalis, a close phylogenetic relative of *Bacteroides* sp., incorporates at least half of the total 3-hydroxy *iso*branched $C_{17:0}$ into complex lipids other than lipopolysaccharide (3). HPLC fractionation of complex lipids isolated from *P. gingivalis* demonstrated several fractions containing 3-hydroxy *iso*branched $C_{17:0}$ (3). Of the major lipid fractions containing 3-hydroxy *iso*branched $C_{17:0}$, the lipid fraction with highest mobility (least polarity) contains 3-hydroxy *iso*branched $C_{17:0}$ in amide linkage but lacks phosphorus, free amine, or choline and migrates close to mammalian ceramide standard on silica gel thin-layer chromatography (unpublished results). In contrast to the ceramide phospholipids identified by other investigators, this evidence suggests the presence of a ceramide lipid. Complex lipids extracted from diseased gingival tissue also include a major nonpolar lipid fraction containing 3-hydroxy *iso*branched $C_{17:0}$ (3). Although *P. gingivalis* is considered to be a significant periodontal pathogen, it is unknown whether bacterial ceramides exist in diseased gingival tissue and whether bacterial ceramides participate in the pathogenesis of periodontal disease. The purpose of the present study was first to characterize the ceramide lipids recovered from *P. gingivalis* using gas chromatography–mass spectrometry and second to determine whether these characteristic lipids of *P. gingivalis* are recovered in lipid extracts from diseased tooth root surfaces and in lipids extracted from diseased gingival tissues.

Abbreviations: HPLC, high pressure liquid chromatography; PFB, pentafluorobenzyl; TMS, trimethylsilyl; GC, gas chromatography.

MATERIALS AND METHODS

Teeth and gingival tissue samples were obtained in the Periodontology and Oral and Maxillofacial Surgery Clinics at the University of Connecticut School of Dental Medicine. Teeth from severe adult periodontitis disease sites were frozen immediately after extraction without removal of adherent gingival tissue or soft and mineralized bacterial deposits. Gingival tissue samples were excised during routine periodontal surgical procedures from severe adult periodontitis sites and were immediately frozen until processing. Severe periodontitis sites demonstrated greater than 50% bone and attachment loss, bacterial plaque and calculus, and severe gingival inflammation. *P. gingivalis*, grown in pure culture and lyophilized, was generously provided by Dr. Paulette Tempro, Department of Periodontics, State University of New York at Buffalo. Sphingosine (d(+)-*erythro*-2-amino-4-*trans*-octadecene-1,3,diol), ceramide (N-stearoyl-d-sphingosine), and fatty acid standards were purchased from Matreya, Inc., Pleasant Gap, PA. Dihydrosphingosine standards (d,l-*erythro*-2-amino-1,3-octadecanediol and d-*threo*-2-amino-1,3-octadecanediol) were purchased from Sigma Chemical Co., St. Louis, MO.

Lipid extraction from *P. gingivalis*, teeth and gingival tissue

Lipids of *P. gingivalis* were extracted using a modification of the phospholipid extraction procedure of Bligh and Dyer (13, 14). Approximately 4 g of lyophilized bacterial pellet was extracted by adding 16 ml of methanol–chloroform 2:1 (v/v) and 4 ml of water. The sample was vortexed and allowed to stand for 2 h. Chloroform (6 ml) and 2 N KCL + 0.5 N K_2HPO_4 (6 ml) were then added and the mixture was vortexed. After gaining phase separation with centrifugation (1000 *g*, 10 min), the lower organic phase was removed and the resultant complex lipids were dried under nitrogen. Teeth (n = 7), removed from a patient due to severe adult periodontitis, were subjected to the same lipid extraction procedure. Frozen gingival tissue samples (approximately 4 g, wet weight) were pooled, minced, and placed in an ice-cold glass tube containing ice-cold methanol (6 ml). Tissue samples were then homogenized using a Polytron homogenizer. The homogenate was then supplemented with 6 ml methanol, 6 ml chloroform, and 3 ml of water. After standing for 2 h, chloroform (4.5 ml) and 2 N KCL + 0.5 N K_2HPO_4 (4.5 ml) were added. After vortexing and centrifuging (1000 *g*, 10 min), the lower organic phase (lipid phase) was removed and the organic extract was dried and stored under nitrogen at −20°C until further processing.

Hydrolysis of lipid samples and sample processing

A sample of *P. gingivalis* lipid (1 mg) was subjected to alkaline hydrolysis (4 N KOH, 100°C, 2 h). For most experiments, the alkaline hydrolyzate was extracted with chloroform (2 × 2 ml) in order to recover long chain bases and the chloroform extract was washed twice with water (2 ml). The aqueous washings were returned to the alkaline hydrolyzate and the sample was made acidic (pH < 1) with concentrated HCl. The acidified sample was extracted with hexane (2 × 2 ml) to recover fatty acids, the hexane extract was combined with the chloroform extract, and the combined organic solvent extract was dried under nitrogen. When recovery of long chain bases was not essential, the alkaline hydrolyzate of *P. gingivalis* lipid was acidified with concentrated HCl and the fatty acids were extracted into chloroform (2 × 2 ml).

Hydrogenation of lipid extracts

Approximately 1 mg of *P. gingivalis* lipid was subjected to alkaline hydrolysis and fatty acids were recovered. The fatty acids were dissolved in 5 ml of spectral grade methanol containing 1 mg of platinum oxide and hydrogenated by bubbling H_2 through the sample at 50°C for at least 2 h. After hydrogenation, the methanol was dried under a stream of N_2 and the lipids were extracted with chloroform (2 × 1 ml).

Derivative synthesis for gas chromatography–mass spectrometry

A sample of complex lipid extract (approximately 1 mg each) from *P. gingivalis*, teeth, and gingival tissue were treated overnight with N,O-bis(trimethylsilyl)-trifluoroacetamide (50 μl) and heated for 1 h at 60°C. Each sample was then transferred to a microvial and sealed with Teflon-lined crimp cap.

For negative ion chemical ionization–mass spectrometry, the combined long chain base and fatty acid extracts were dissolved in acetonitrile (30 μl) and treated with 35% pentafluorobenzylbromide in acetonitrile (10 μl) and diisopropylethylamine (10 μl). The solution was heated for 20 min at 40°C and evaporated to dryness under nitrogen. The resultant pentafluorobenzyl esters and amines were then treated with N,O-bis(trimethylsilyl)-trifluoroacetamide (50 μl) and incubated overnight followed by heating for 1 h at 60°C. Each sample was then transferred to a microvial and sealed with a Teflon-lined crimp cap.

For electron impact–mass spectrometry of bacterial fatty acids, samples were treated with N,O-bis(trimethylsilyl)-trifluoroacetamide (50 μl) overnight. For electron impact–mass spectrometry of bacterial long chain bases combined with fatty acids, the sample was treated overnight with 2% methoxyamine hydrochloride in pyridine (50 μl), dried under nitrogen, and treated overnight with N,O-bis(trimethylsilyl)-trifluoroacetamide (50 μl). Each sample was then transferred to a microvial and sealed with a Teflon-lined crimp cap.

Gas chromatography–mass spectrometry analysis

The lipid derivatives were analyzed using a Hewlett-Packard 5890 gas chromatograph interfaced with a 5988A mass spectrometer. Samples of complex lipid extracts were applied to an SPB-1 column (0.1 mm film × 0.25 mm × 15 m, Supelco, Inc., State College, PA). Complex lipid samples were injected with the inlet block at 310°C using the splitless mode with a temperature program of 10°C/min from 200°C to 300°C followed by 5°C/min to 310°C and 4 min at 310°C. The mass spectrometer was used in the electron impact ionization mode with the ion source temperature of 200°C, an electron energy of 70 eV, and an emission current of 300 mA.

Long chain base and fatty acid derivatives were applied to the Ultra-1 column (0.33 mm film × 0.2 mm × 12 m, Hewlett-Packard, Avondale, PA) using the splitless mode with the inlet block maintained at 100°C. The temperature was increased at 10°C/min to 170°C followed by 5°C/min to 270°C. When the mass spectrometer was used in the negative ion–chemical ionization mode, the ion source temperature was 100°C with an electron energy of 240 eV and an emission current of 300 mA. Methane was used as reagent gas at 0.5 torr. When the mass spectrometer was used in the electron impact ionization mode, the ion source temperature was 150°C with an electron energy of 70 eV and an emission current of 300 mA.

Hazardous procedures

The derivatizing agents used in this study were used only in a high efficiency fume hood and care was taken to prevent exposure of these agents to water or aqueous solvents. Rubber gloves were worn to protect hands and skin from exposure to these derivatizing agents.

RESULTS

The separation of *P. gingivalis* complex lipids by gas chromatography revealed four major peaks as well as sev-

eral minor peaks as demonstrated in the uppermost chromatogram of **Fig. 1**. The partial mass spectra (m/z 200–800) for each major lipid peak are listed according to the peak retention time. Two peaks exhibit mass spectra consistent with ceramide structures containing 3-hydroxy $C_{17:0}$ in amide linkage with either 2-amino-1,3-nonadecanediol (retention time = 11.937 min) or 2-amino-1,3-octadecanediol (retention time = 11.514 min) (**Fig. 2**). However, peaks with retention times of 11.023 and 10.562 min reveal mass spectra which suggest either *1*) a double bond between carbons 1 and carbon 2 of monohydroxylated long chain bases (18 or 19 carbons in length) linked to 3-hydroxy $C_{17:0}$, or *2*) a double bond between carbon 2 and carbon 3 of a $C_{17:1}$ fatty acid linked to dihydroxy saturated long chain bases (18 or 19 carbons in length). The latter structures are depicted in **Fig. 3**.

The fatty acid and long chain base constituents of *P. gingivalis* lipids were evaluated next. A method was developed to detect long chain bases and fatty acids simultaneously by forming pentafluorobenzyl, trimethylsilyl derivatives of long chain bases and fatty acids and applying negative ion chemical ionization of the gas chromatographic separated products. This method has been used extensively for fatty acid detection. Verification of the method for long chain base detection was accomplished using synthetic sphingosine standard (d(+)-*erythro*-2-amino-4-*trans*-octadecene-1, 3-diol). The sphingosine standard was treated with pentafluorobenzyl bromide followed by N,O-bis(trimethylsilyl)-trifluoroacetamide as described in the Materials and Methods. **Figure 4** shows the total ion chromatogram of this derivative and the characteristic negative ion chemical ionization mass spectra. A single major peak with a base peak ion mass of m/z 513 was detected. Electron impact mass spectrometry of the pentafluorobenzyl, trimethylsilyl derivative failed to detect this peak (data not shown). Furthermore, negative ion chemical ionization mass spectrometry of the trimethylsilyl derivative of spingosine also failed to detect this peak (data not shown). Therefore, the

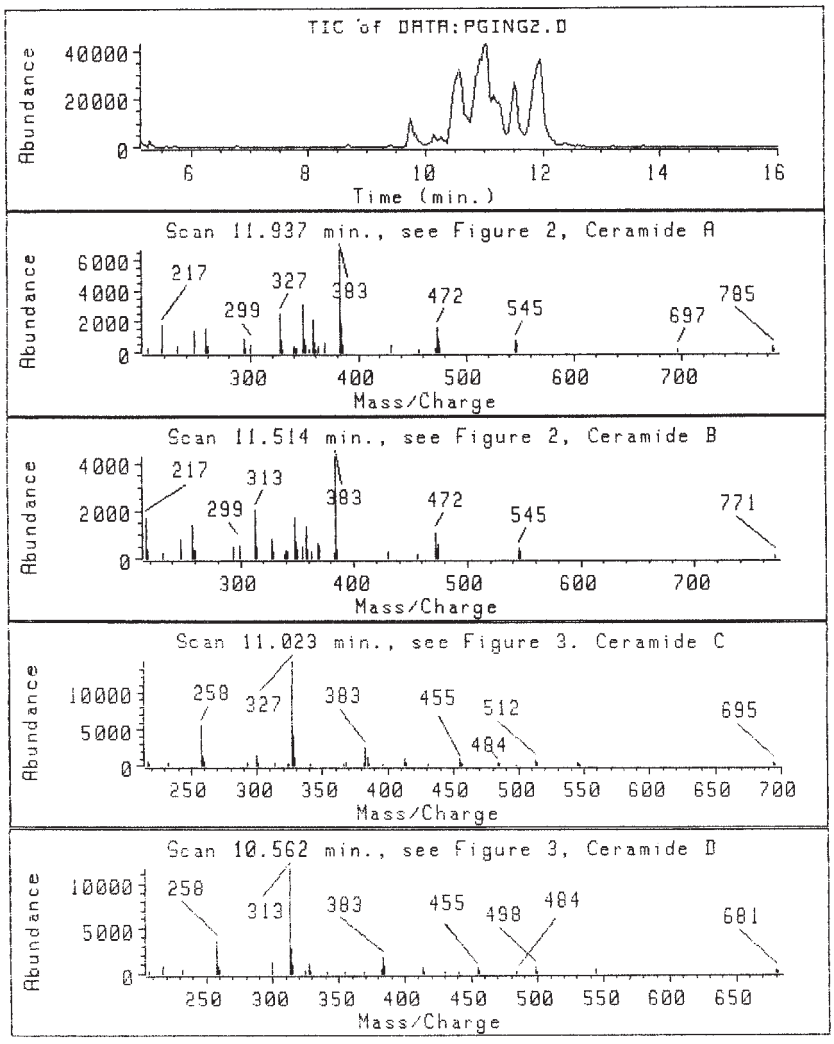

Fig. 1. Ceramides recovered in complex lipid extracts from *P. gingivalis*. Lipids were extracted from *P. gingivalis* and treated to form trimethylsilyl derivatives. The gas chromatographic separation and mass spectrometer detector characteristics are described in the Materials and Methods. The uppermost figure represents the total ion chromatogram (TIC) and the partial mass spectra listed below represent major ceramide peaks designated by the respective retention times. Mass spectra were acquired using a range of m/z 200 to 800.

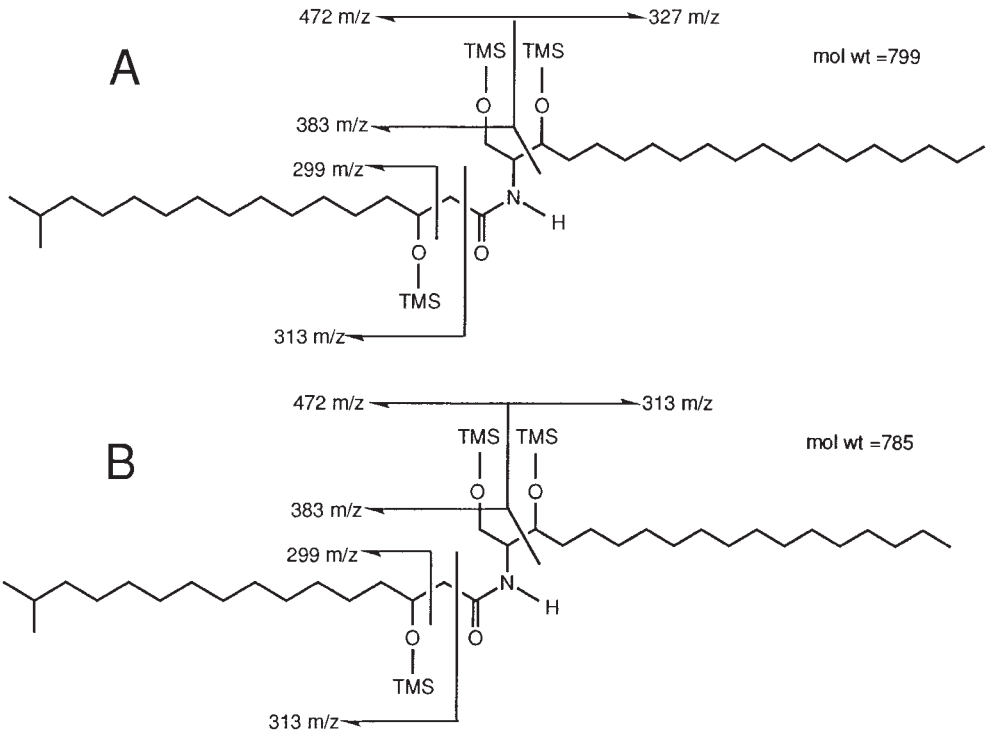

Fig. 2. Proposed structures of two major ceramides recovered from *P. gingivalis*. Ceramides A and B correspond to the GC peaks in Fig. 1 with retention times of 11.937 min and 11.514 min, respectively.

ionized sphingosine derivative product detected by negative ion chemical ionization is proposed to result from loss of the pentafluorobenzyl moiety from the nitrogen with formation of a double bond.

A sample of *P. gingivalis* lipid was subjected to alkaline hydrolysis and the recovered long chain bases and fatty acids were treated to form pentafluorobenzyl, trimethylsilyl derivatives as described in the Materials and Methods.

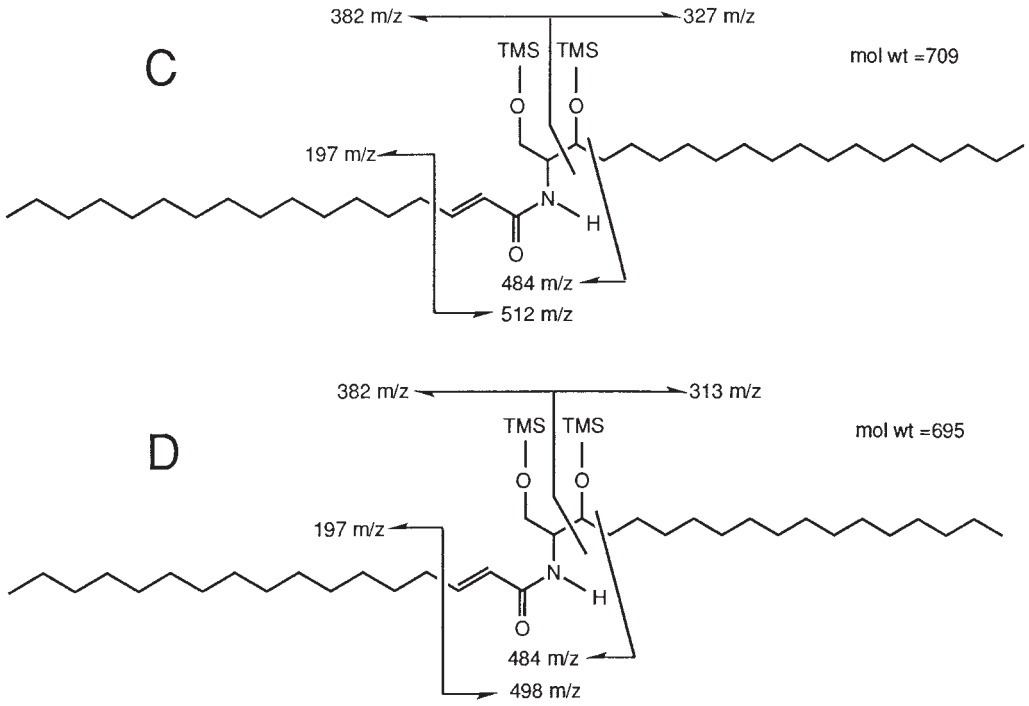

Fig. 3. Proposed structures of two unusual ceramides recovered from *P. gingivalis*. Ceramides C and D correspond to the GC peaks in Fig. 1 with retention times of 11.023 min and 10.562 min, respectively.

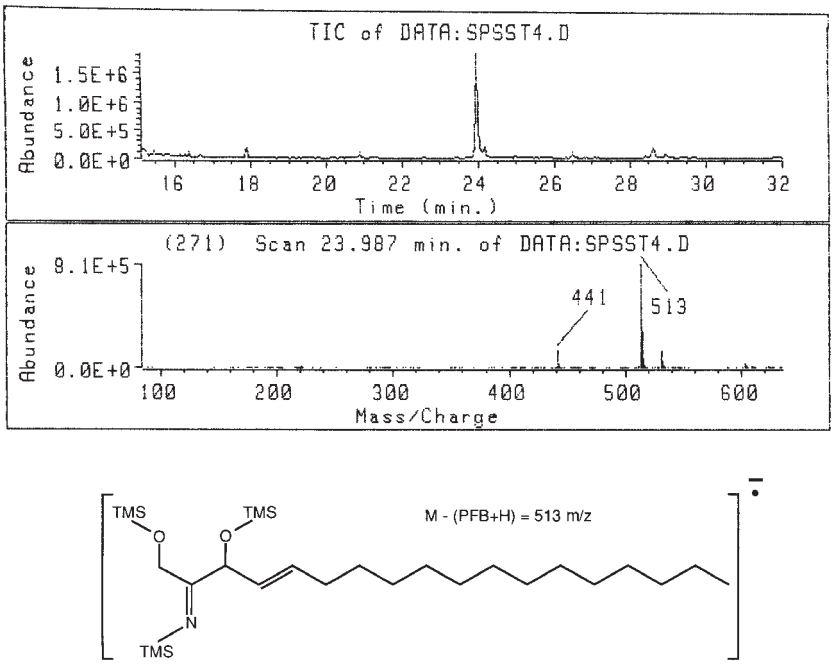

Fig. 4. Gas chromatographic recovery and mass spectra of sphingosine standard. Sphingosine standard (d(+)-*erythro*-2-amino-4-*trans*-octadecene-1,3-diol) was derivatized and analyzed as described in the Materials and Methods. The upper chromatogram represents the total ion chromatogram (TIC) of the sphingosine standard under which is the negative ion chemical ionization spectra of the major peak and the proposed derivative structure detected.

The chromatogram at the top of **Fig. 5** demonstrates the gas chromatographic separation of hydrolysis products. The negative ion chemical ionization mass spectra are depicted by retention time of gas chromatographic peaks of interest and are listed in the order of elution from the column (starting with the peak at 25.000 min). Based on retention times and characteristic base peak ion spectra of known fatty acid standards, the following products were identified: the peak at 19.309 min with a mass spectral base peak ion of m/z 267 is predicted to be $C_{17:1}$; the peak at 20.903 min with a base peak ion of m/z 357 comigrates with 3-hydroxy *iso*branched $C_{17:0}$ standard; the peak at 22.230 min with a base peak ion of m/z 501 is predicted to be 2-amino-1,3-heptadecanediol; the peak at 24.057 min with a base peak ion of m/z 515 comigrates with d,l-*erythro*-2-amino-4-*trans*-octadecane-1,3,diol standard; and the peaks at 24.883 and 25.000 min with a base peak ions of m/z 529 are predicted to be isomeric forms of 2-amino-1,3-nonadecanediol. No products were identified indicating the presence of 2-amino-1-octadecene-3-ol or 2-amino-1-nonadecene-3-ol in lipids of *P. gingivalis*. If monounsaturated long chain bases are present in *P. gingivalis* lipids, they are not prevalent relative to the saturated long chain bases.

An additional sample of *P. gingivalis* lipid was subjected to alkaline hydrolysis and the long chain bases and fatty acids were recovered. The lipid sample was treated to form methoxime, trimethylsilyl derivatives as described in the Materials and Methods. The chromatogram at the top of **Fig. 6** demonstrates the separation of trimethylsilyl derivatives of long chain bases using electron impact mass spectrometry. The electron impact mass spectra are depicted for peaks of interest by retention time and are listed in the order of elution from the column (starting with the peak at 15.374 min). The following products were identified: the peak at 13.781 min has a mass spectra consistent with a structure of 2-amino-1,3-heptadecanediol; the peak at 14.854 has a mass spectra consistent with a structure of 2-amino-1,3-octadecanediol; and the peak at 15.374 min has a mass spectra consistent with a structure of 2-amino-1,3-nonadecanediol. The proposed fragmentation of long chain base derivatives is listed below the mass spectra. The peak at 14.854 min coelutes with the trimethylsilyl derivative of d,l-*erythro*-2-amino-1,3-octadecanediol standard and demonstrates mass spectral characteristics identical to the standard (data not shown). The trimethylsilyl derivative of d-*threo*-2-amino-1,3-octadecanediol elutes approximately 0.35 min earlier than the *erythro* derivative, indicating that 2-amino-1,3-octadecanediol exists in the *erythro* epimer in *P. gingivalis* ceramides. Future experiments will evaluate these structural aspects within the remaining long chain bases. The mass spectra of long chain bases in Fig. 6 are consistent with long chain base structures predicted by the mass spectra in Fig. 5. Furthermore, the absence of methoxime derivatives indicates that ketone residues are absent from *P. gingivalis* long chain bases.

The analysis of fatty acid from *P. gingivalis* lipids is shown in **Fig. 7**. Fatty acids of *P. gingivalis* lipids were recovered after alkaline hydrolysis and treated to form trimethylsilyl derivatives. The chromatogram at the top of Fig.

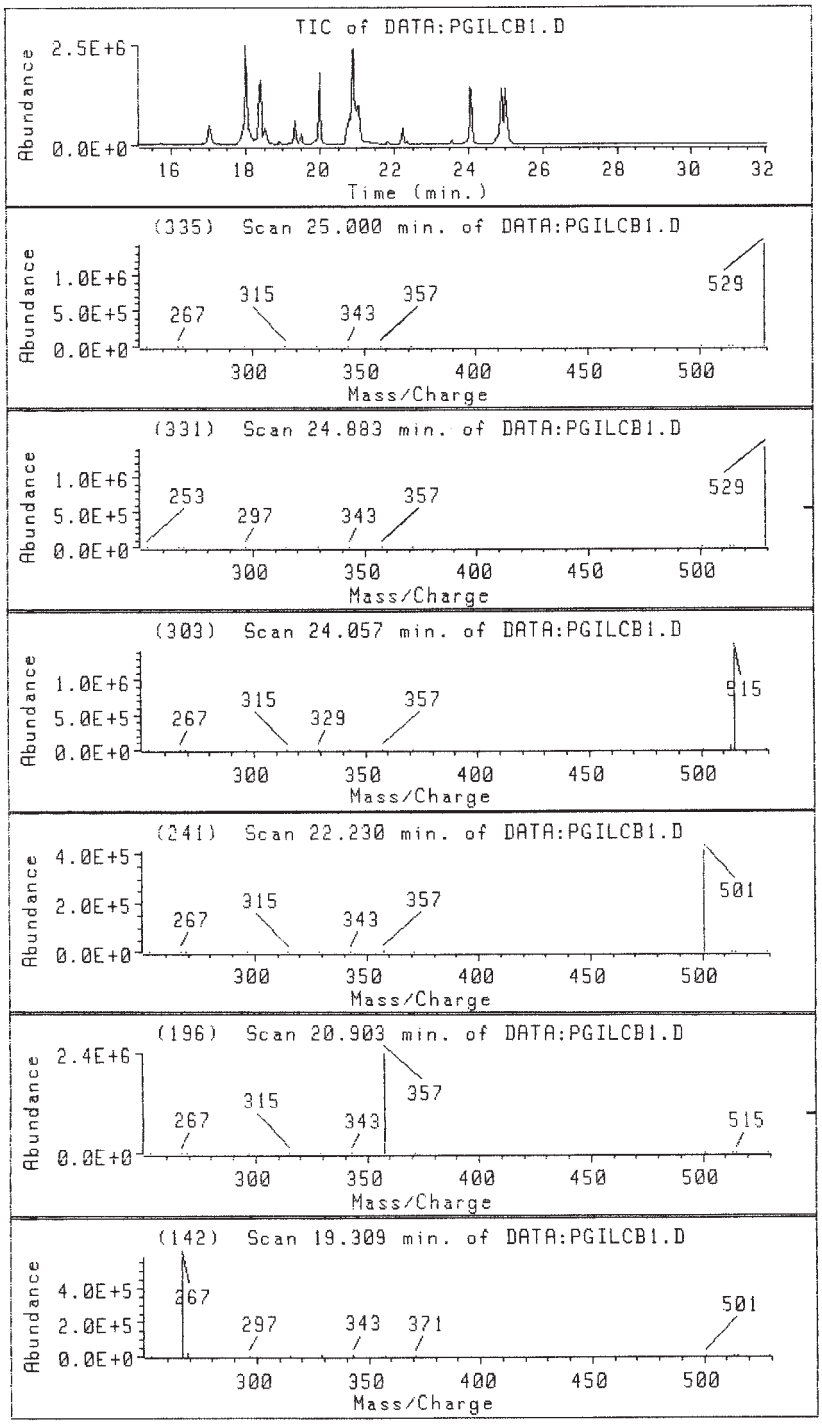

Fig. 5. Fatty acids and long chain bases recovered from lipids of *P. gingivalis* after alkaline hydrolysis. A sample of *P. gingivalis* lipid was processed and analyzed as described in the Materials and Methods. The uppermost figure demonstrates the total ion chromatogram (TIC) of the hydrolytic products of *P. gingivalis* lipids. The corresponding negative ion chemical ionization spectra are depicted for selected major peaks in the total ion chromatogram according to the corresponding retention times.

7 demonstrates the separation of trimethylsilyl derivatives of fatty acids using electron impact mass spectrometry. *P. gingivalis* fatty acids of interest were identified by the peak retention time and characteristic mass spectra. The peak eluting at 12.770 min has a mass spectra and retention time consistent with 3-hydroxy *iso*branched $C_{17:0}$ standard (**Fig. 8**). Straight-chained 3-hydroxy $C_{17:0}$ standard elutes at 13.072 min (Fig. 8). However, the peak eluting at 13.083 min in Fig. 7 represents an unknown fatty acid which is clearly different from 3-hydroxy *iso*branched $C_{17:0}$ or 3-hydroxy $C_{17:0}$ (mass spectra not shown). The peak eluting at 11.589 min in Fig. 7 has a mass spectra consis-

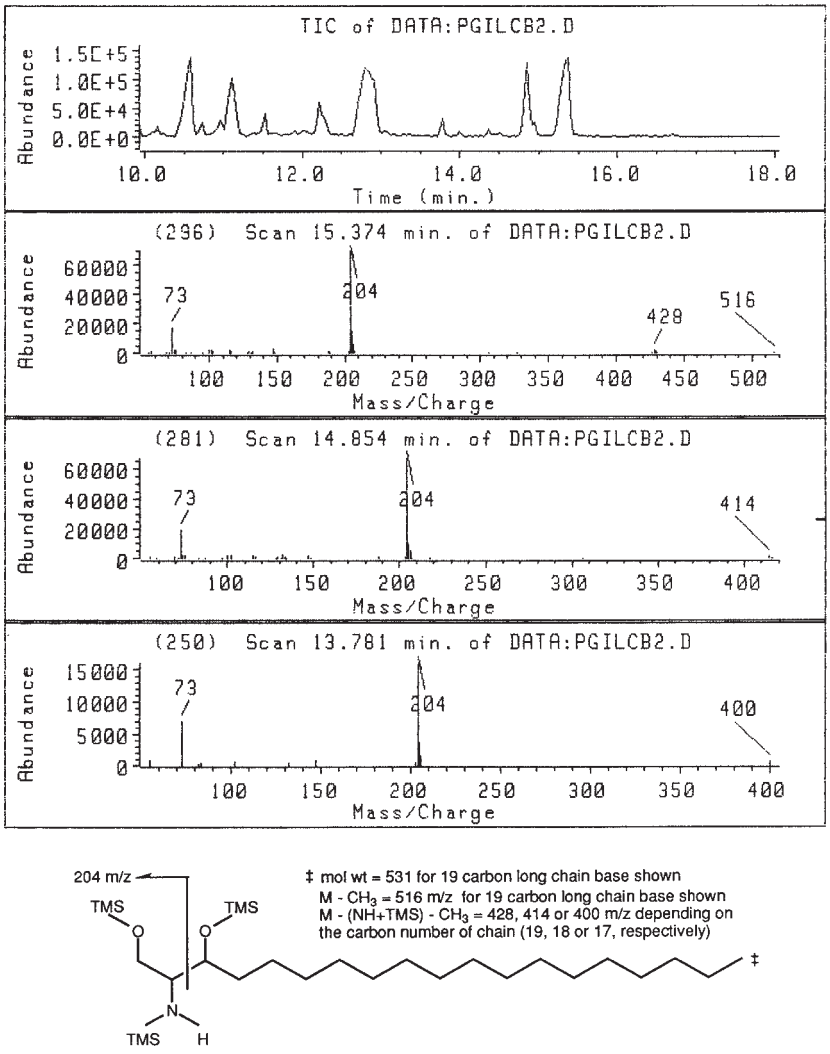

Fig. 6. Trimethylsilyl derivatives of long chain bases recovered from lipids of *P. gingivalis* after alkaline hydrolysis. A sample of *P. gingivalis* lipid was hydrolyzed as described in the Materials and Methods and the long chain bases were extracted into chloroform. The recovered long chain bases were first treated overnight with 2% methoxyamine hydrochloride in pyridine (50 μl), dried and treated overnight with N,O-bis(trimethylsilyl)-trifluoroacetamide (50 μl). The uppermost figure demonstrates the total ion chromatogram (TIC) of the long chain bases derivatives of *P. gingivalis* lipids. The corresponding electron impact spectra are depicted only for long chain base peaks in the total ion chromatogram according to the corresponding retention times. Absence of methoxime residues in the bacterial long chain derivatives and fatty acid derivatives indicates that ketone groups are not present.

tent with a structure of $C_{17:1}$. The double bond location in $C_{17:1}$ was confirmed by examining the mass spectra of $C_{16:1}$ standard (2(E)-hexadecenoic acid). The trimethylsilyl derivative of $C_{16:1}$ showed a major ion peak at m/z 143 (Fig. 8) as well as other low molecular weight fragments associated with cleavage around the α–β double bond. The 143 m/z ion product was not observed in mass spectra of the trimethylsilyl derivative of $C_{16:0}$ (Fig. 8). This evidence strongly supports the conclusion that the double bond in $C_{17:1}$ of *P. gingivalis* lipids is located between carbon 2 and carbon 3. The peaks eluting at 11.527 min and 12.811 min in Fig. 6 show mass spectra identical to those depicted in Fig. 7.

The double bond in the $C_{17:1}$ fatty acid peak was further verified by hydrogenating fatty acids recovered from hydrolyzed *P. gingivalis* lipids. *P. gingivalis* lipid (approximately 1 mg) was subjected to alkaline hydrolysis and the fatty acids were recovered. The fatty acid extract was hydrogenated and treated to form pentafluorobenzyl derivatives. **Figure 9** shows the selected ion chromatograms for unhydrogenated fatty acids (upper frame) compared with the hydrogenated fatty acids (lower frame). Hydrogenation of the fatty acids recovered from *P. gingivalis* substantially reduced the recovery of peaks in the m/z 267 ion scan when compared with peaks recovered in the m/z 269 ion scan.

Using selected ion monitoring for characteristic high molecular weight ions of ceramides from *P. gingivalis* (**Fig. 10**), teeth removed from sites afflicted with severe adult periodontitis were shown to contain lipids corresponding

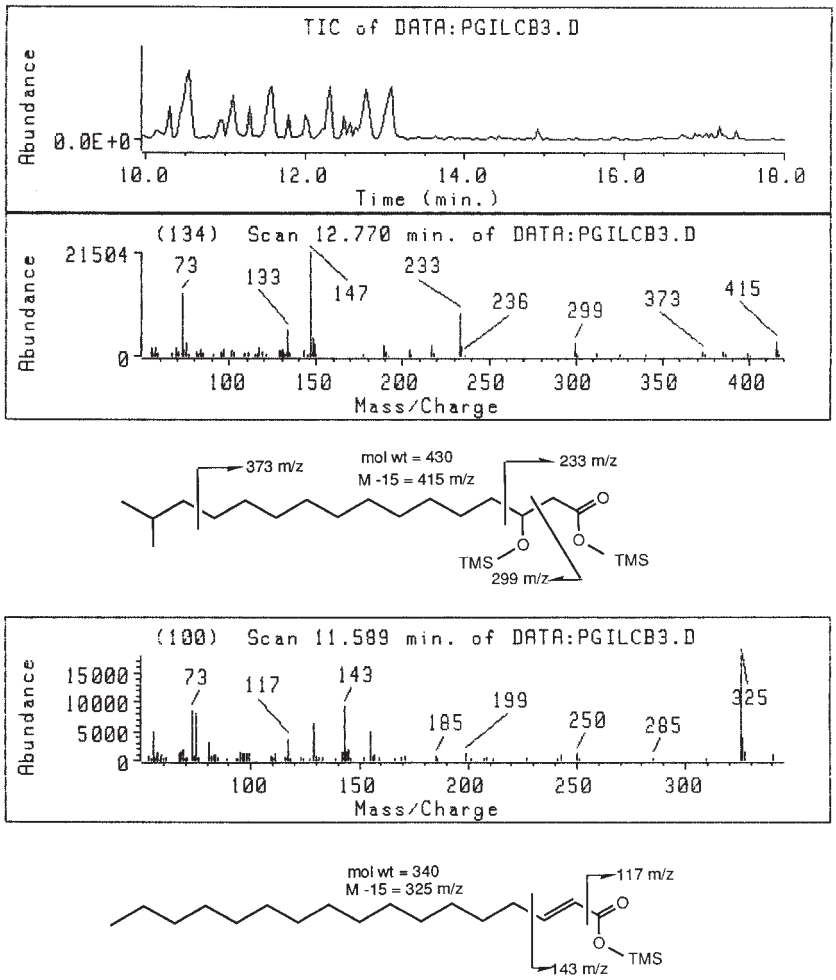

Fig. 7. Trimethylsilyl derivatives of selected fatty acids recovered from lipids of *P. gingivalis* after alkaline hydrolysis. A sample of *P. gingivalis* lipid was hydrolyzed as described in the Materials and Methods and fatty acids were extracted into chloroform after acidification of the hydrolyzate. The recovered fatty acids were treated overnight with N,O-bis(trimethylsilyl)-trifluoroacetamide (50 μl). The uppermost figure demonstrates the total ion chromatogram (TIC) of the fatty acids recovered from P. *gingivalis* lipids. The corresponding electron impact spectra and structures are depicted for trimethylsilyl derivatives of 3-hydroxy *iso*-branched $C_{17:0}$ and $C_{17:1}$.

to the four major ceramide products identified in *P. gingivalis* lipids (Fig. 1). However, the lower molecular weight ceramides recovered from *P. gingivalis* (corresponding to ions of *m*/*z* 681 and 695) predominated in lipid extracts from diseased teeth. The higher molecular weight ceramides with corresponding ions of *m*/*z* 771 and 785 were substantially less abundant when compared with the lower molecular weight ceramides. The peak retention time for each product was shifted approximately 0.2 min earlier than was observed in Fig. 1, presumably due to the reduced ceramide content of the teeth lipid sample.

Selected ion monitoring of lipid extracts from diseased gingival tissue samples revealed *m*/*z* 327, 383, and 512 ion peaks coincident with the *m*/*z* 695 peak shown in Fig. 10 (data not shown). Ion peaks for *m*/*z* 383 and 498 were also coincident with the *m*/*z* 681 ion peak shown in Fig. 10, although these ion peaks were relatively low in abundance (data not shown). Finally, characteristic ions representative of the higher molecular weight ceramides shown in Fig. 10 were not observed in this gingival tissue lipid extract.

DISCUSSION

The present report is the first to demonstrate the general structural characteristics of trimethylsilyl derivatives of ceramides from *P. gingivalis*. Previous reports demonstrated the feasibility of detecting trimethylsilyl derivatives of ceramides (15–18) using large bore packed columns coated with 1% OV-1, a nonpolar exchangeable phase. The characteristic mass spectra of trimethylsilyl-ether derivatives of synthetic ceramides were reported as well (15, 17, 18) and are structurally consistent with those shown in Fig. 1. Capillary gas chromatographic columns interfaced to a mass spectrometer offer many advantages over packed columns including good sample detection with minimal

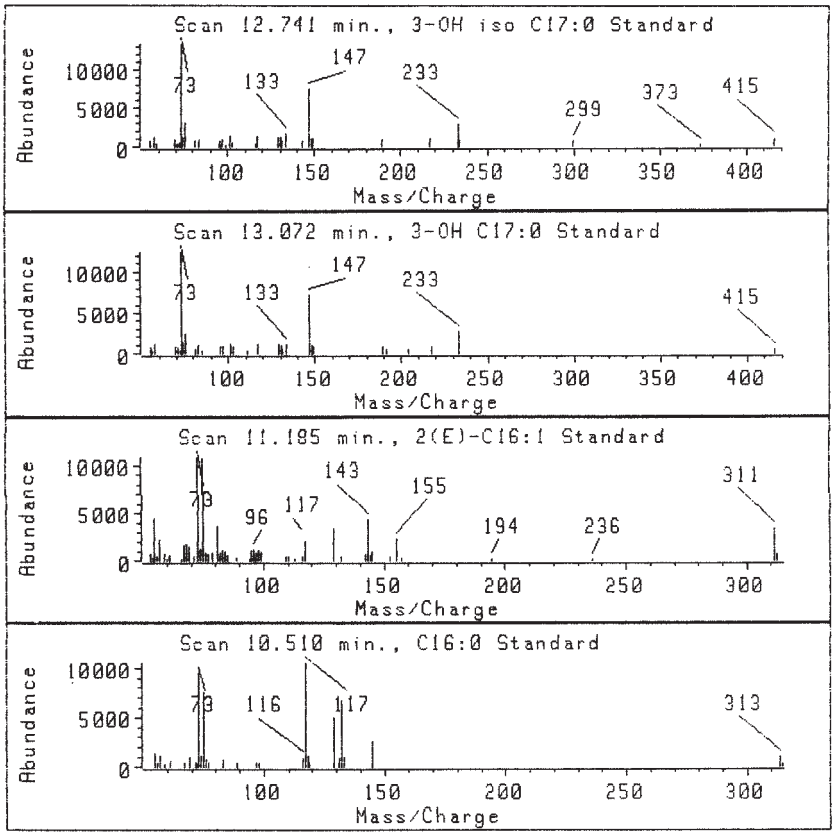

Fig. 8. Trimethylsilyl derivatives of fatty acids standards. Fatty acid standards were treated to form trimethylsilyl derivatives as described in the Materials and Methods. Electron impact mass spectra are depicted for the following fatty acid standards: 3-hydroxy *iso*branched $C_{17:0}$, 3-hydroxy $C_{17:0}$, $C_{16:1}$ (2(E)-hexenoic acid), and $C_{16:0}$.

sample mass applied to the column, high sample resolution, and low bleed of cross-linked phases. However, the recovery of trimethylsilyl derivatives of ceramides from the Ultra-1 capillary column proved to be somewhat problematic even though the exchangeable phase of an Ultra-1 column is equivalent in polarity to the 1% OV-1 phase used in early studies (15–18). This was presumed to occur because the poly(dimethylsiloxane) bonded phase of the Ultra-1 column is thick (0.33 mm) which results in low yields and prolonged retention of high molecular weight ceramide derivatives. The poly(dimethylsiloxane) SPB-1 capillary column (0.1 mm film thickness) provided considerably higher yields of ceramide derivatives although individual ceramide peaks were not resolved as well when compared with the ceramide separations on an Ultra-1 column. Because a primary goal of this study was to obtain mass spectral characteristics of ceramides for structural analysis, the SPB-1 column was used in order to maximize the introduction of bacterial ceramides into the mass spectrometer.

Two complex lipids recovered from *P. gingivalis* demonstrate mass spectral characteristics consistent with the ceramide structures shown in Fig. 2. These proposed ceramide structures (A) and (B) correspond to the gas chromatographic peaks with retention times of 11.937 min and 11.514 min, respectively, shown in Fig. 1. The mass spectra of synthetic ceramides described by others (15–18) suggest that the high mass ions for ceramides A and B most likely represent the m/z M–15$^+$ products of the respective ceramide derivatives. Repeated attempts to recover the m/z M$^+$ ions for the depicted ceramides were unsuccessful, primarily because this ion is present in low abundance and the mass spectrometer is not equipped with a high mass detector. Note that the ion masses round up by one atomic mass unit at masses greater than m/z 650. In fact, the tabulated mass spectra reveal the high mass ions to be m/z 770.75 and m/z 784.75 for the proposed ceramides (A) and (B), respectively. Many of the lower molecular weight ion products shown in Fig. 2 also correspond to comparable fragmentation products demonstrated by others using synthetic ceramide standards (15–18). The m/z 545 ion results from cleavage between C-2 and C-3 of the long chain base and simultaneous transfer of a trimethylsilyl residue from the C-3 carbon to the nitrogen, as reported by others (15, 17, 18).

The long chain base moieties of ceramides A and B are shown as straight chains of either 18 carbons (2-amino-1,3-octadecanediol is represented as the GC peak with a retention time = 24.057 min in Fig. 5 or the GC peak with a retention time of 14.854 min in Fig. 6) or 19 carbons (2-amino-1,3-nonadecanediol). Additional analysis using

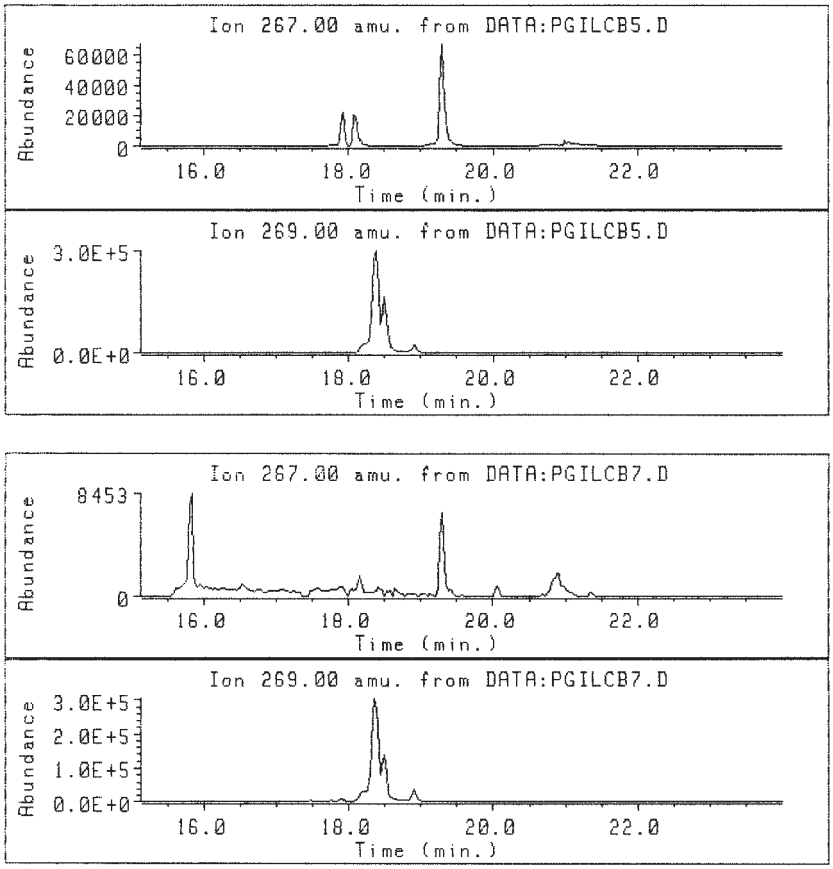

Fig. 9. Hydrogenation of $C_{17:1}$ recovered from *P. gingivalis*. A lipid sample (approximately 1 mg) from *P. gingivalis* was subjected to alkaline hydrolysis and the fatty acids were recovered. The fatty acid sample was hydrogenated as described in the Materials and Methods and treated to form pentafluorobenzyl ester derivatives. Each frame depicts selected ion monitoring of $C_{17:1}$ (m/z 267) and $C_{17:0}$ (m/z 269). The upper frame represents unhydrogenated fatty acids whereas the lower frame represents hydrogenated fatty acids.

erythro and *threo* standards of 2-amino-1,3-octadecanediol revealed that the 18 carbon long chain base of *P. gingivalis* exists in the *erythro* epimer. It is likely that the 19 carbon long chain base molecules exist in the *erythro* epimer as well. However, the 19 carbon long chain base may also exist as both straight-chain and *iso*branched forms because two peaks with a base peak ion of m/z 529 were noted in Fig. 5 (GC peak retention times of 25.000 min or 24.883 min). By contrast, the trimethylsilyl derivative of the 19 carbon long chain base from *P. gingivalis* did not reveal two peaks (Fig. 6, GC peak retention time = 15.374 min). Further evaluation of P. *gingivalis* long chain bases using acetyl, trimethylsilyl derivatives revealed that acetylation of the amine is accompanied by partial acetylation of the hydroxyl group on carbon 1 of the long chain base. This leads to formation of two derivatives for each long chain base. However, the 19 carbon long chain base demonstrated two peaks for the diacetyl, trimethylsilyl derivative and only one peak for the acetyl, ditrimethylsilyl derivative (data not shown). Regardless of the basis for this isomerization, the base peak ions of m/z 515 and 529 (Fig. 5) as well as the long chain bases identified in Fig. 6, are consistent with the predicted masses of the previously characterized long chain base molecules identified in *Bacteroides melaninogenicus* (12). The *iso*branched form of 2-amino-1,3-nonadecanediol (17-methyl octadecasphinganine), but not straight-chain 2-amino-1,3-nonadecanediol, was recovered in ceramide phospholipids isolated from *B. melaninogenicus* (12). Future research will attempt to clarify these structural issues for *P. gingivalis* ceramides.

Ceramides A and B shown in Fig. 2 are proposed to contain amide-linked 3-hydroxy *iso*branched $C_{17:0}$. Analysis of hydrolysis products of *P. gingivalis* lipids demonstrated the recovery of 3-hydroxy *iso*branched $C_{17:0}$ as either a pentafluorobenzyl-ester, trimethylsilyl-ether derivative (Fig. 5, GC peak retention time = 20.903 min, base peak ion = m/z 357) or as a trimethylsilyl-ester, trimethylsilyl-ether derivative (Fig. 7, GC peak retention time = 12.770 min). That *P. gingivalis* lipids contain 3-hydroxy *iso*branched $C_{17:0}$ was verified using a commercially available standard (Fig. 8). Therefore, the constituent long chain bases and hydroxy fatty acid for ceramides A and B (depicted in Figs. 5–8) are recovered in alkaline hydrolyzates of *P. gingivalis* lipids.

The additional major complex lipid peaks eluting with retention times of 11.023 min and 10.562 min in Fig. 1 correspond to ceramide structures C and D, respectively, shown in Fig. 3. Although the mass spectra shown in Fig. 1

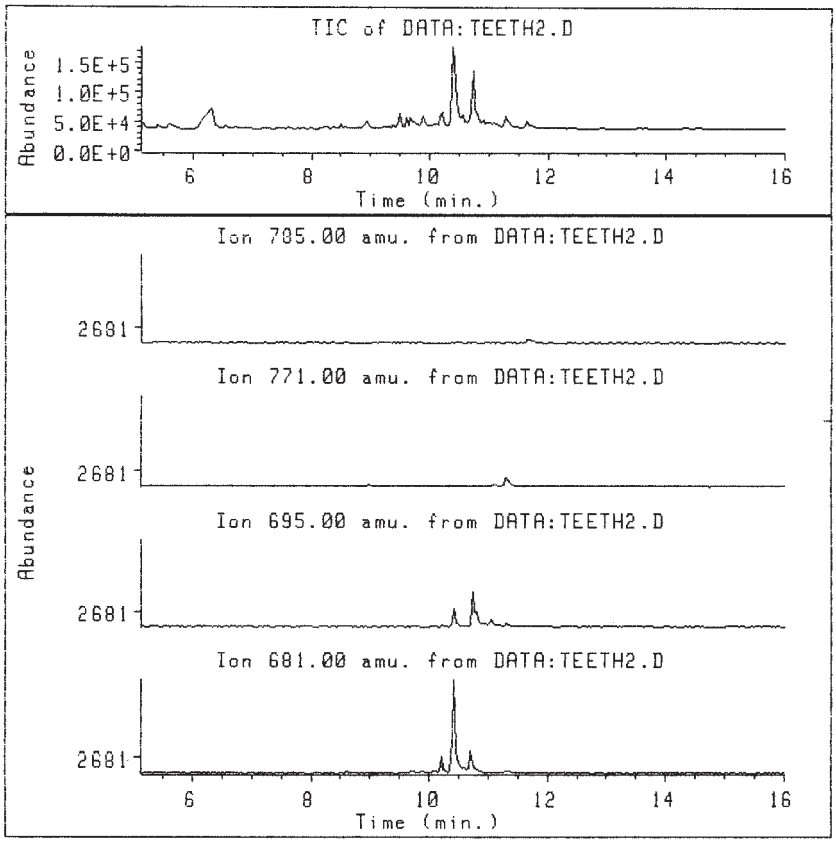

Fig. 10. Ceramides from teeth afflicted with severe adult periodontitis. The lipid extraction from teeth, preparation of lipid derivatives, and gas chromatography–mass spectrometry procedures are described in the Materials and Methods. The uppermost figure represents the total ion chromatogram (TIC) of lipids extracted from teeth. The selected ion monitoring chromatograms listed below the total ion chromatogram demonstrate the recovery of m/z M–15$^+$ ions characteristic of ceramides described in Fig. 1.

could be consistent with ceramides containing monounsaturated, monohydroxy long chain bases linked to 3-hydroxy *iso*branched $C_{17:0}$, analysis of hydrolysis products from *P. gingivalis* lipids failed to demonstrate monohydroxy long chain bases with a double bond between carbon 1 and carbon 2. In fact, the only additional long chain base peak identified was 2-amino-1,3-heptadecanediol (Fig. 5, GC peak with a retention time of 22.230 min and Fig. 6, GC peak with a retention time of 13.781 min). All other major products in the chromatograms from Figs. 5 and 6 represent fatty acids. Included in these fatty acids was $C_{17:1}$ either as a pentafluorobenzyl-ester derivative (Fig. 5, GC peak retention time = 19.309 min, base peak ion = m/z 267) or as a trimethylsilyl-ester derivative (Fig. 7, GC peak retention time = 11.589 min). Furthermore, hydrogenation of alkaline hydrolysis products of *P. gingivalis* lipids dramatically reduced the recovery of gas chromatographic peaks on the m/z 267 ion scan (Fig. 9) further supporting the presence of an unsaturated C_{17} fatty acid within *P. gingivalis* lipids. Therefore, it is proposed that $C_{17:1}$ in amide linkage to the previously described bacterial long chain bases (2-amino-1,3-octadecanediol and 2-amino-1,3-nonadecanediol) accounts for the ceramide structures shown in Fig. 3.

There are some important differences between the mass spectra shown in Fig. 2 and those shown in Fig. 3. The tabulated mass spectra for ceramides C and D show low abundance of the m/z 382 ion (20–30%) relative to the abundance of the m/z 383 ion. Cleavage between C-2 and C-3 of the long chain base of ceramides C and D is associated with preferential proton addition to the nitrogen. That the 382 fragment is correctly represented in Fig. 3 is supported by the recovery of an m/z 455 ion (the m/z 455 ion abundance is approximately 50% of the m/z 383 ion) which results from cleavage between C-2 and C-3 with trimethylsilyl transfer from C-3 to the nitrogen. Loss of the 197 fragment from the 455 ion yields an m/z 258 ion. Further support for the proposed structures comes from the m/z 484 ion (the m/z 484 ion abundance is approximately 30% of the m/z 383 ion abundance). The m/z 484 ion is proposed to occur with cleavage between carbon 3 and carbon 4 of the long chain base for both ceramides C and D.

Verification of the proposed bacterial ceramide structures required both negative ion chemical ionization and electron impact mass spectrometry of fatty acids and long chain bases recovered after alkaline hydrolysis of *P. gingivalis* lipids. Although both methods are routinely used for detection of fatty acids, application of negative ion chemical ionization to detect pentafluorobenzyl-amine, trimethylsilyl-ether derivatives of long chain bases provides high

sensitivity in detecting m/z [M – (PFB + H)]$^-$ ion products. Application of this method in detecting synthetic sphingosine standard is shown in Fig. 4. The proposed pentafluorobenzyl-amine, trimethylsilyl-ether derivative of sphingosine was detected only with negative ion chemical ionization and was not detected with electron impact ionization. Furthermore, negative ion chemical ionization of the trimethylsilyl-amine, trimethylsilyl-ether derivative of sphingosine did not reveal an m/z [M–H]$^-$ ion, indicating that the pentafluorobenzyl derivative must be formed to detect long chain bases by negative ion chemical ionization. In addition, the mass spectra shown in Fig. 4 indicate one pentafluorobenzyl substitution on sphingosine presumably because steric hindrance prevents formation of a tertiary amine with double pentafluorobenzyl substitution. Treatment of pentafluorobenzyl-sphingosine with N,O-bis(trimethylsilyl)-trifluoroacetamide is proposed to form trimethylsilyl-ethers at hydroxyl groups and a pentafluorobenzyl, trimethylsilyl tertiary amine. This derivative rearranges under negative ion–chemical ionization to form the product shown in Fig. 4. It is possible that the amine is substituted only with a pentafluorobenzyl group, representing a secondary amine, and that intermolecular reactions under negative ion chemical ionization lead to attack of the nitrogen by a trimethylsilyl residue with subsequent double bond formation. However, mass spectral analysis of the small gas chromatographic peak following the primary peak at 23.987 min in Fig. 4 demonstrated a base peak ion of m/z 441 (data not shown). This peak probably represents the pentafluorobenzyl-secondary amine derivative which reacts under negative ion chemical ionization in the same manner as the primary derivative product. Finally, derivatization of increasing amounts of sphingosine versus a $C_{19:0}$ internal standard revealed a linear quantitative recovery of sphingosine derivative (data not shown). Further support for the proposed structure shown in Fig. 4 comes from the m/z 515 (A + 2 isotope ratio) and 514 (A + 1 isotope ratio) ions which predict a structure containing 2.7 silicon atoms and 18.1 carbons, respectively (data not shown). Therefore, this new method provides a sensitive method for detecting long chain bases simultaneously with fatty acid products within biological samples.

The central structure of the ceramides shown in Fig. 3 is interesting because the double bond will likely demonstrate resonance delocalization with the amide bond, thereby protecting the fatty acid double bond from reduction with hydrogenation. This conclusion is reached because long-term hydrogenation of bacterial ceramides (overnight at 50°C) did not alter their mass spectra and did not alter the recovery of $C_{17:1}$ after alkaline hydrolysis of hydrogenated *P. gingivalis* lipids (data not shown). Significant reduction of the $C_{17:1}$ recovery was demonstrated only when the fatty acids of *P. gingivalis* were first released by alkaline hydrolysis and subsequently hydrogenated (Fig. 9). In addition, virtually complete double bond saturation of linoleic acid and synthetic sphingosine standards occurred after hydrogenation for 2 h (data not shown). Therefore, the proximity of the fatty acid double bond to the amide bond in ceramides depicted in Fig. 3 results in reduced chemical reactivity of the double bond which may impact on the biological properties of these lipids when present in mammalian tissues.

Selected ion monitoring for the characteristic m/z M–15$^+$ ions of the ceramides shown in Figs. 2 and 3 revealed that teeth from severe adult periodontitis sites harbor significant levels of ceramide lipids predominantly of the type shown in Fig. 3 (m/z ions of 681 and 695). The ceramide lipids shown in Fig. 2 (m/z ions of 771 and 785) were considerably less prevalent in the lipid samples from teeth. Selected ion monitoring for the most characteristic ions shown in Fig. 3 demonstrated coincident recovery with the m/z M–15$^+$ ions of ceramides C and D (data not shown). This evidence indicates that adult periodontitis is associated with the accumulation of ceramide lipids of bacterial origin on diseased root surfaces and that the unusual ceramides depicted in Fig. 3 may be preferentially adsorbed over other bacterial ceramides. Although ceramides A and B (Fig. 2) are considerably less abundant than ceramides C and D on these diseased root surfaces, 3-hydroxy *iso*-branched $C_{17:0}$ is present on diseased root surfaces as a constituent of bacterial ceramide. A previous report concluded that recovery of 3-hydroxy $C_{17:0}$ on diseased root surfaces reflects the presence of lipid A of bacterial lipopolysaccharide (19). The evidence provided in this report indicates that 3-hydroxy *iso*branched $C_{17:0}$ recovered on diseased root surfaces may be a constituent of bacterial ceramides as well.

Although a previous report demonstrated 3-hydroxy *iso*-branched $C_{17:0}$ in diseased gingival tissue within a limited group of complex lipids (3), the identity of these complex lipids was not established. The evidence described in the present report indicates that the recovery of 3-hydroxy *iso*-branched $C_{17:0}$ in diseased gingival tissue reflects in part the penetration of specific bacterial ceramides presumably synthesized by *P. gingivalis* and other related organisms. That the unusual ceramides recovered in *P. gingivalis* are selectively recovered on teeth and in diseased gingival tissue suggests that bacterial ceramides adsorbed to diseased root surfaces may penetrate through direct contact with gingival cells. The fact that bacteria containing 3-hydroxy *iso*branched $C_{17:0}$ are not recovered in significant levels within diseased gingival tissue (3) suggests that the presence of periodontal microorganisms may have little bearing on the lipid penetration process other than to provide the ceramide lipid for adsorption to root surfaces. Additional research is needed to examine this relationship as well as to examine the biological activities of these ceramides as potential mediators of periodontal destruction. Finally, the recently discovered properties of ceramides to act as biological signaling agents (20–24) may be relevant to the presence of bacterial ceramides on teeth root surfaces and in diseased gingival tissues.

In summary, the present report describes the basic structural characteristics of four major ceramides in *P. gingivalis* and demonstrates the presence of these ceramides on diseased teeth. In addition, at least two of these bacte-

rial ceramides are recovered in diseased gingival tissues. Further research is needed to clarify the importance of these bacterial ceramides in periodontal tissue function and their role in periodontal disease pathogenesis.

I thank Dr. Paulette Tempro, Department of Periodontics, State University of New York at Buffalo, for providing bacterial samples for this study, and Dr. John Schenkman, Department of Pharmacology, University of Connecticut, School of Medicine, for his assistance in the hydrogenation reactions. I also thank faculty and residents of the Departments of Oral and Maxillofacial Surgery and Periodontology for their assistance in obtaining teeth and gingival tissue samples used in this study. I also thank Dr. John Dean for his critical evaluation of this manuscript. Finally, I thank Dr. Clarence Trummel for his financial assistance in supporting these studies.

Manuscript received 9 July 1998.

REFERENCES

1. Johne, B., and K. Bryn. 1986. Chemical composition and biological properties of a lipopolysaccharide from *Bacteroides intermedius*. *Acta Pathol. Microbiol. Immunol. Scand. Sect. B.* **94:** 265–271.
2. Johne, B., I. Olsen, and K. Bryn. 1988. Fatty acids and sugars in lipopolysaccharides from *Bacteroides intermedius*, *Bacteroides gingivalis*, and *Bacteroides loescheii*. *Oral Microbiol. Immunol.* **3:** 22–27.
3. Nichols, F. C. 1994. Distribution of 3-hydroxy iC17:0 in subgingival plaque and gingival tissue samples: relationship to adult periodontitis. *Infect. Immun.* **62:** 3753–3760.
4. Shah, H. N., and M. D. Collins. 1983. Genus *Bacteroides*: a chemotaxonomical perspective. *J. Appl. Bacteriol.* **55:** 403–416.
5. Mayberry, W. R. 1980. Hydroxy fatty acids in *Bacteroides* species: d-(−)-3-hydroxy-15-methylhexadecanoate and its homologs. *J. Bacteriol.* **143:** 582–587.
6. Mayberry, W. R. 1980. Cellular distribution and linkage of d-(−)-3-hydroxy fatty acids in *Bacteroides* species. *J. Bacteriol.* **144:** 200–204.
7. Kunsman, J. E. 1973. Characterization of the lipids of six strains of *Bacteroides ruminicola*. *J. Bacteriol.* **113:** 1121–1126.
8. Rizza, V., A. N. Tucker, and D. C. White. 1970. Lipids of *Bacteroides melaninogenicus*. *J. Bacteriol.* **101:** 84–91.
9. Smith, R. D., and A. A. Salyers. 1981. Incorporation of leucine into phospholipids of *Bacteroides thetaiotaomicron*. *J. Bacteriol.* **145:** 8–13.
10. White, D. C., and A. N. Tucker. 1970. Ceramide phosphorylglycerol phosphate: a new sphingolipid found in bacteria. *Lipids.* **5:** 56–62.
11. Miyagawa, E., R. Azuma, and T. Suto. 1974. Distribution of sphingolipids in *Bacteroides* species. *J. Gen. Microbiol.* **24:** 341–348.
12. White, D. C., A. N. Tucker, and C. C. Sweeley. 1969. Characterization of the *iso*-branched sphinganines from the ceramide phospholipids of *Bacteroides melaninogenicus*. *Biochim. Biophys. Acta.* **187:** 527–532.
13. Bligh, E. G., and W. J. Dyer. 1959. A rapid method of total lipid extraction and purification. *Can. J. Biochem. Physiol.* **37:** 911–917.
14. Garbus, J., H. F. DeLuca, M. E. Loomas, and F. M. Strong. 1968. Rapid incorporation of phosphate into mitochondrial lipids. *J. Biol. Chem.* **238:** 59–63.
15. Hammarström, S. 1970. Gas–liquid chromatography–mass spectrometry of synthetic ceramides containing phytosphingosine. *J. Lipid Res.* **11:** 175–182.
16. Samuelsson, B., and K. Samuelsson. 1968. Gas–liquid chromatographic separation of ceramides as di-O-trimethyl-silyl ether derivatives. *Biochim. Biophys. Acta.* **164:** 421–423.
17. Samuelsson, B., and K. Samuelsson. 1969. Gas–liquid chromatography–mass spectrometry of synthetic ceramides. *J. Lipid Res.* **10:** 41–46.
18. Hammarström, S., B. Samuelsson, and K. Samuelsson. 1970. Gas–liquid chromatography–mass spectrometry of synthetic ceramides containing 2-hydroxy fatty acids. *J. Lipid Res.* **11:** 150–157.
19. Lygre, H., E. Solheim, N. R. Gjerdet, and N. Skaug. 1992. Fatty acids of healthy and periodontally diseased root substance in human teeth. *J. Dent. Res.* **71:** 43–46.
20. Ballou, L. R., C. P. Chao, M. A. Holness, S. C. Barker, and R. Raghow. 1992. Interleukin-1-mediated PGE_2 production and sphingomyelin metabolism. Evidence for the regulation of cyclooxygenase gene expression by sphingosine and ceramide. *J. Biol. Chem.* **267:** 20044–20050.
21. Dressler, K. A., S. Mathias, and R. N. Kolesnick. 1992. Tumor necrosis factor-α activates the sphingomyelin signal transduction pathway in a cell-free system. *Science.* **255:** 1715–1718.
22. Obeid, L. M., C. M. Linardic, L. A. Karolak, and Y. A. Hannun. 1993. Programmed cell death induced by ceramide. *Science.* **259:** 1769–1771.
23. Tepper, C. G., S. Jayadev, B. Liu, A. Bielawska, R. Wolff, S. Yonehara, Y. Hannun, and M. F. Seldin. 1995. Role for ceramides as an endogenous mediator of Fas-induced cytotoxicity. *Proc. Natl. Acad. Sci. USA.* **92:** 8443–8447.
24. Verheij, M., R. Bose, X. H. Lin, B. Yao, W. D. Jarvis, S. Grant, M. J. Birrer, E. Szabo, L. I. Zon, J. M. Kyriakis, A. Haimovitz-Friedman, Z. Fuks, and R. N. Kolesnick. 1996. Requirement for ceramide-initiated SAPK/JNK signalling in stress-induced apoptosis. *Nature.* **380:** 75–79.